

FOLDER: Accelerating Multi-modal Large Language Models with Enhanced Performance

Haicheng Wang^{1,2*}, Zhemeng Yu^{1,2*}, Gabriele Spadaro^{2,3}, Chen Ju⁴, Victor Quétu², Enzo Tartaglione²✉

¹ SJTU Paris Elite Institute of Technology, Shanghai Jiao Tong University, China

² LTCI, Télécom Paris, Institut Polytechnique de Paris, France

³ University of Turin, Italy ⁴ Alibaba Group, China

{anakin_skywalker, fish_meng}@sjtu.edu.cn, gabriele.spadaro@unito.it,
cju.void@gmail.com, {victor.quetu, enzo.tartaglione}@telecom-paris.fr
<https://github.com/anakin-skywalker-Joseph/Folder>

Abstract

Recently, Multi-modal Large Language Models (MLLMs) have shown remarkable effectiveness for multi-modal tasks due to their abilities to generate and understand cross-modal data. However, processing long sequences of visual tokens extracted from visual backbones poses a challenge for deployment in real-time applications. To address this issue, we introduce **FOLDER**, a simple yet effective plug-and-play module designed to reduce the length of the visual token sequence, mitigating both computational and memory demands during training and inference. Through a comprehensive analysis of the token reduction process, we analyze the information loss introduced by different reduction strategies and develop FOLDER to preserve key information while removing visual redundancy. We showcase the effectiveness of FOLDER by integrating it into the visual backbone of several MLLMs, significantly accelerating the inference phase. Furthermore, we evaluate its utility as a training accelerator or even performance booster for MLLMs. In both contexts, FOLDER achieves comparable or even better performance than the original models, while dramatically reducing complexity by removing up to 70% of visual tokens.

1. Introduction

Multi-modal Large Language Models (MLLMs) have become a powerful framework for multimodal tasks, playing a key role in applications such as image captioning [13] and visual question answering [42]. By learning a joint representation of visual and textual information, state-of-the-art MLLMs like GPT-4V [1] and Claude 3 [2] have demonstrated great capabilities in understanding and even gener-

*: Equation contribution. ✉: Corresponding author.

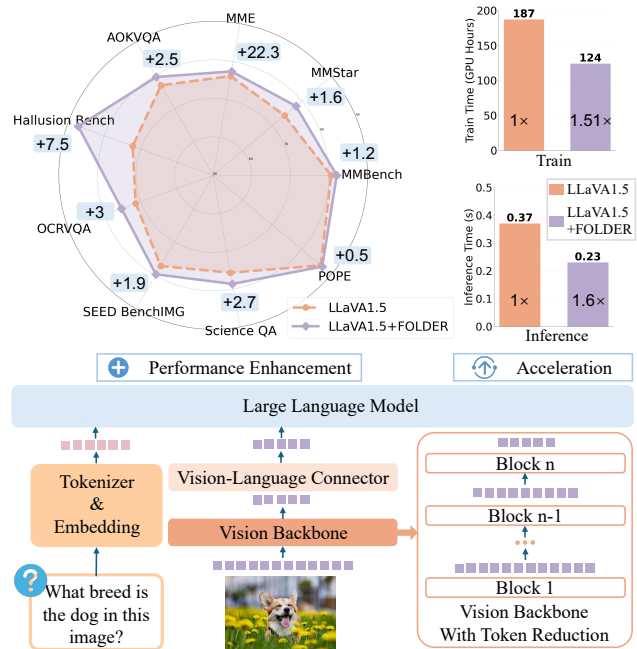


Figure 1. **FOLDER as Accelerator & Booster.** As a plug-and-play module, FOLDER can be used in both training and inference, with considerable acceleration and even performance boost.

ating multimodal content. However, these models face concrete challenges in terms of computational efficiency, particularly when processing visual inputs.

Modern MLLMs typically generate long sequences of image tokens through their visual backbones. In some application scenarios, this problem becomes even more evident: recent advancements in high-resolution-supporting MLLMs [11, 78] might involve over 2000 visual tokens. Similarly, multi-visual-expert architectures [40, 72, 76] leverage multiple visual encoders, encountering analogous

challenges. These issues are even more pronounced in video understanding models [30, 47, 50] due to the temporal dimension of video content. This rapid increase in token sequence length represents a challenge for real-time application deployment due to the *quadratic computational complexity* of the attention mechanism.

Several studies have been conducted to address this issue. Existing approaches can be roughly divided into two categories. The first category focuses on *training phase* solutions, such as Q-Former [46], resampler [11] and pooling-based techniques [6]. However, these methods often suffer from performance degradation and exhibit limited scalability, due to their custom design for specific architectures. The second category aims to design plug-and-play token reduction modules for the *inference phase* [8, 39]. While these methods identify the inherent redundancy in visual tokens, their reduction strategies are often arbitrary, *e.g.* employing a uniform reduction for each layer/block, resulting in sub-optimal outcomes. Specifically, these methods fail to consider the information loss during the token reduction process, thus leading to substantial performance drops.

To find a reduction strategy that can preserve the performance, we propose a preliminary investigation to answer a fundamental question: *Where does information loss originate?* To model it, we identify three key factors that impact information loss during token removal: **Reduction Impact**, **Propagation Effect**, and **Aggregation Method**. Through a comprehensive empirical study of these factors, we devise a strategy that enhances the preservation of information while significantly reducing redundancy. FOLDER is consequently designed to implement this strategy with minimal computational overhead. Our plug-and-play solution can be seamlessly integrated into the visual backbones of various MLLMs, effectively reducing the number of visual tokens while incurring negligible information loss (Fig. 1). We first incorporate FOLDER during MLLMs inference, reducing over 60% of visual tokens and achieving comparable, or even gains on performance across multiple tasks. Furthermore, when integrated into MLLMs pre-training, our module can be used as a training accelerator, as well as an effective regularization term, leading to remarkable performance improvements across all benchmarks, with a reduction ratio up to 70%. Our method is on-the-field proven to be a flexible, nearly lossless, and highly efficient token reduction strategy, offering a dual-purpose solution to the visual token reduction challenge. In summary, our contributions can be summarized as:

- We conduct an in-depth analysis for the sources of information decay during token reduction, identifying and quantifying the key factors involved (Sec. 3.1, Sec. 3.2 and Sec. 3.3). These insights offer a clear understanding of how token reduction impacts the information flow.
- Leveraging the above analysis, we develop a simple yet

effective plug-and-play visual token reduction module for MLLMs (Sec. 3.4). This novel token reduction strategy aggressively reduces the number of tokens only in the last blocks of the visual encoder. On various models and benchmarks, FOLDER speeds up the inference 1.7-2.4× with negligible loss or even improvement (Sec. 4.2.1).

- We demonstrate that our method can also be useful in MLLM training (Sec. 4.2.2), improving both the performance and the speed.

2. Related Works

Multi-modal Large Language Models have gained considerable attention due to the powerful ability to understand multi-modality effectively [1, 3, 6, 46, 48, 50, 52, 73–75, 78, 87], and can thus benefit lots of downstream tasks: image domain [9, 10, 14, 15, 60–63, 77, 82, 83], video domain [12, 31–35, 37, 38, 89], as well as audio domain [55–58]. A popular MLLM architecture for vision is composed of i.) Visual Backbone, ii.) Vision-Language Connector and iii.) Pre-trained Large Language Model. The integration of visual information leads to rapid growth in computational cost due to the large number of visual tokens. For instance, LLaVA1.5 [54] employs 576 tokens for a 336×336 image and up to several thousands of tokens for high-resolution images. This issue becomes even more obvious for video understanding models [30, 47, 50]. For instance, in VideoLLaVA [50], even when performing inference with a limited 8 frames at a resolution of 224×224 , the sequence length already surpasses 2000 tokens. Recently, some works [40, 72, 76] demonstrate the importance of using multiple complementary vision towers to enhance MLLMs’ visual ability. While effective, this approach even aggravates the sequence length issue.

MLLMs Acceleration. Many approaches focus on system-level optimizations for acceleration, such as FlashAttention [17], vLLM [16], and RingAttention [53]. Techniques on knowledge distillation [22, 79], quantization [23, 80] and model pruning [67, 71, 79] were also introduced to reduce model size and computational cost. However, these approaches fail to address the challenge of redundant data, which leads to unnecessarily long sequences.

Token Reduction in MLLMs. Some preliminary studies are conducted on token reduction for Vision Transformers [5, 43, 49]. In the context of MLLMs, several token reduction methods, including Q-Former [46], resampler [11] and pooling [6] are proposed to reduce visual tokens during the training process. However, these approaches often suffer from performance degradation and lack of scalability.

Meanwhile, some studies try to handle the token reduction problem during inference. In particular, ToMe [5] proposes a training-free token merging strategy for uni-modal image classification. Based on that, Turbo [36, 39] proposes

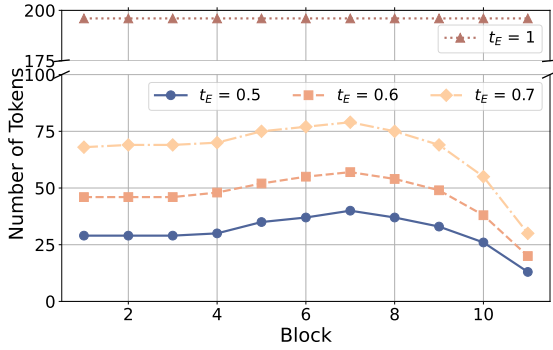


Figure 2. **Minimum Number of Tokens with Energy t_E Across Blocks.** We evaluate on three types of t_E for every block.

an improved merging strategy considering both mutual redundancy and semantic value, serving as a plug-in module in MLLMs. Recently, FastV [8] recognizes the visual attention sparsity in LLM, thus pruning visual tokens inside the LLM based on the task-orientated attention importance. Though effective, these methods have clear drawbacks. For ToMe/Turbo, the uniform progressive merging across all layers is arbitrary and inflexible, while FastV mainly suffers from two major problems: i.) FastV requires the attention map for every output token, so the kv-cache needs to keep the visual tokens throughout the whole dialogue, making it unsuitable for long-term visual QA. ii.) Since FastV is inserted in LLM, it is difficult to adapt for complex LLM modules [17]. To address these issues, we seek to find an effective, information-guided, and user-friendly token reduction method that can be applied without constraints. Note that there are some concurrent works [29, 70, 81, 88] on MLLM token reduction.

3. Method

In this section, we ground our FOLDER by first answering three key questions for token reduction: i.) how many tokens to reduce (Sec. 3.1); ii.) in which block (Sec. 3.2); iii.) through which aggregation method (Sec. 3.3). Then, we present our method in Sec. 3.4.

Empirical Setup. To answer these three crucial questions, we define a common empirical setup. Specifically, we use a pre-trained 12-block ViT-B [19] model and conduct the empirical experiments on ImageNet-1k [18]. Results on more diverse setups are provided in supplementary materials.

3.1. Token Reduction Impact

To investigate the intuitive relation between the reduced number of tokens and information drop, we leverage the Singular Value Decomposition (SVD) to monitor the energy of one reduced token sequence. Given a token sequence

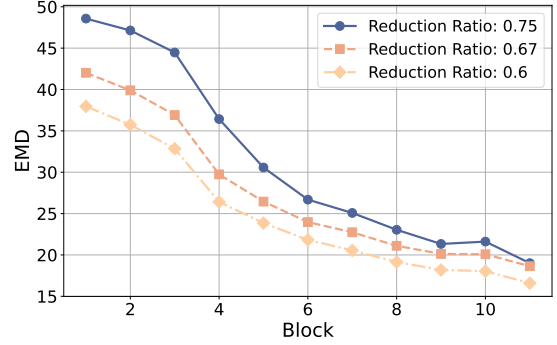


Figure 3. **EMD Distance Between Reduced and Original Output Distributions under 3 Reduction Ratios.** We compare the EMD distance by exerting token reduction on different blocks.

$\mathbf{X} \in \mathbb{R}^{n \times d}$ (with n being the number of tokens and d their size), we can decompose it applying SVD on \mathbf{X}^T :

$$\mathbf{X}^T = \mathbf{U}\mathbf{\Sigma}\mathbf{V}^T, \quad (1)$$

where $\mathbf{U} \in \mathbb{R}^{d \times d}$ and $\mathbf{V} \in \mathbb{R}^{n \times n}$ are two orthogonal matrices and $\mathbf{\Sigma} \in \mathbb{R}^{d \times n}$ is a diagonal matrix, with the singular values $\sigma_i = \mathbf{\Sigma}_{ii}$ representing the variances (energy) in the new compositional directions. In this way, SVD yields the *optimal* energy concentration that can be ordered by their contribution to the total variance (energy) [20]. Based on this, we can estimate how much variance we preserve by only taking the largest k singular values, as:

$$E(k) = \frac{\sum_{i=1}^k \sigma_i}{\sum_{i=1}^n \sigma_i}, \quad \sigma_i \geq \sigma_{i+1} \quad \forall i. \quad (2)$$

By the above definition, SVD provides an *upper bound* on the amount of energy preserved by keeping k tokens. Therefore, by setting a threshold t_E of energy to be conserved, we can estimate the theoretical number of tokens k needed for each block as:

$$k = \min\{k \mid E(k) \geq t_E\}. \quad (3)$$

Observations. Setting a threshold t_E , k changes across different blocks. To evaluate the potential token reduction, we use our empirical setup to monitor the change in k (once t_E is defined) in different blocks of the model. As shown in Fig. 2, to preserve the same amount of energy, later blocks require significantly fewer tokens than earlier ones. These results offer key indications for developing block-adaptive token reduction strategies, suggesting that the first and last blocks might be suitable candidates.

3.2. Token Propagation Effect

While token reduction impact offers an upper bound for information preservation, this approximation does not account for inter-block dependencies and therefore may not

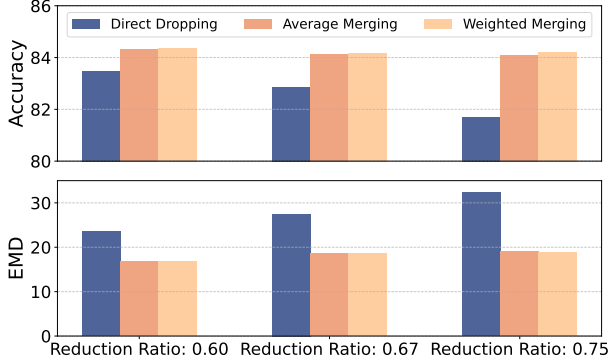


Figure 4. **Comparison of EMD and Accuracy for Aggregation Methods.** We compare “direct dropping”, “average merging” and “weighted merging” under different reduction ratios.

adequately reflect the effects on subsequent blocks. Indeed, due to the sequential structure of transformer architectures, errors introduced by token reduction from former blocks can propagate through the network. Similar to the butterfly effects, this impact can accumulate or even amplify through successive modules and non-linear transformations [4], thus influencing the final performance.

To analyze this propagation effect, we examine how token reduction at different blocks affects the final output distribution. Thus, by comparing the original output token distribution (without reduction) and the one obtained by operating token reduction only in one block b , we can show the presence of such a propagation effect.

To measure this distortion, we consider output tokens from the original model $\mathbf{Y} \in \mathbb{R}^{n \times d}$ and the ones obtained when $n - k$ tokens are reduced in the block b : $\tilde{\mathbf{Y}}_b \in \mathbb{R}^{k \times d}$. Then, we define the empirical distributions P_Y and $P_{\tilde{Y}_b}$ supported on \mathbf{Y} and $\tilde{\mathbf{Y}}_b$ respectively, and we evaluate Earth Mover’s Distance (EMD) [68] between them:

$$\text{EMD}(P_Y, P_{\tilde{Y}_b}) = \min_{\gamma} \langle \gamma, \mathbf{M} \rangle_F, \quad (4)$$

where $\mathbf{M} = (d_{ij})_{n \times k} = (\|y_i - \tilde{y}_{bj}\|_2)_{n \times k}$ denotes the metric cost matrix, with y_i and \tilde{y}_{bj} being points in the support of distributions P_Y and $P_{\tilde{Y}_b}$ respectively. $\gamma = (\gamma_{ij})_{n \times k}$ represents the optimal transport matrix, which satisfies the non-negative constraint $\gamma_{ij} \geq 0, \forall i, j$ and the marginal constraints $\sum_{j=1}^k \gamma_{ij} = P_Y(y_i)$ and $\sum_{i=1}^n \gamma_{ij} = P_{\tilde{Y}_b}(\tilde{y}_{bj})$.

Observations. Due to the propagation effect, the token reduction operation exerting on different blocks can cause distinct levels of distortion on the output distribution. We thus monitor EMD (4) when the same number of tokens is reduced in each specific block. As evidenced in Fig. 3, reducing tokens in early blocks results in substantially higher EMD values compared to later ones. This observation empirically confirms the presence of such propagation effect,

where the distortion is amplified across the layers of the network. For this reason, first blocks are finally not suitable for token reduction, different from what is suggested in Fig. 2. On the other hand, Fig. 3 shows that even with an aggressive reduction ratio of 75%, EMD remains remarkably low in the last layers. Synthesizing these findings on reduction impact and propagation effect, we conclude that token reduction should be strategically applied at the end of the network, which allows a high degree of reduction. Results on BLIP [45] provided in Tab. 7 confirm these conclusions. More results supporting these observations are provided in supplementary materials.

3.3. Token Aggregation Method

In Sec. 3.1, we leverage SVD to compute the upper bound for information preservation. However, due to the computational complexity of SVD, it cannot be directly applied for token reduction. Thus, leveraging what is done in previous works [5, 39], we decompose this operation into two stages: i.) Token Matching: grouping tokens according to a specific matching function, and ii.) Token Aggregation: consolidating the grouped tokens into a reduced number of tokens. While these works [5, 39] offered insights on matching functions, the latter stage is barely studied. More formally, given a set of tokens $\{\mathbf{x}_1, \mathbf{x}_2, \dots, \mathbf{x}_m\}$ that are expected to be aggregated into a new token \mathbf{y} , we formulate the aggregation operation as follows:

$$\mathbf{y} = \sum_{i=1}^m \alpha_i \mathbf{x}_i, \text{ s.t. } \sum_{i=1}^m \alpha_i = 1. \quad (5)$$

Based on Eq. (5), we formulate three different token aggregation approaches: i.) Average Merging, with $\alpha_i = \frac{1}{m}, \forall i$; ii.) Weighted Merging, with $\alpha_i = \frac{\|x_i\|_2}{\sum_{j=1}^m \|x_j\|_2}, \forall i$; iii.) Direct Dropping, with $\alpha_i = 0, \forall i \neq i_{max}, \alpha_{i_{max}} = 1$ where $i_{max} = \underset{i}{\text{argmax}} \|x_i\|_2$. Here the norm $\|\cdot\|_2$ is used as the importance score for tokens.

Observations. Similarly with Sec. 3.2, we compare these different aggregation methods leveraging the EMD (4). In Fig. 4, we notice that with both merging methods we obtain lower discrepancy compared to the Direct Dropping method. Given that Average Merging achieves comparable results to Weighted Merging with greater simplicity, we select it as our preferred aggregation method. Moreover, we can notice that a lower EMD corresponds to higher final accuracy. More results supporting these observations are provided in Tab. 8 and in supplementary materials.

3.4. FOLDER

Motivation. Based on empirical analyses, we deduce that: i.) Token reduction should take place in the last blocks, where aggressive reduction is permitted. ii.) Merging is better than Dropping for aggregation. Therefore, our goal is to

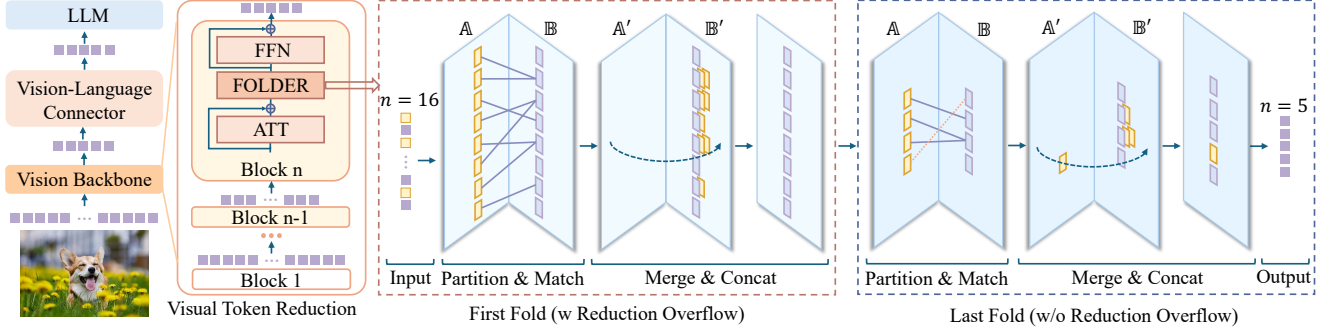


Figure 5. **Pipeline of FOLDER.** As a plug-and-play module, FOLDER is integrated into the final blocks of the vision backbone (last two here). To deal with reduction overflow, FOLDER automatically executes another FOLD operation when the expected reduction is more than half. The last FOLD, which escapes from reduction overflow, merges tokens according to the remaining reduction numbers.

design an algorithm that can reduce as many tokens as possible in one block. Previous works on token merging mainly use bipartite matching [5], which is limited by a maximum reduction ratio of $1/2$. Thus, to aggressively reduce tokens in one block, we propose *FOLDER*, a new bipartite matching strategy that can reduce an arbitrary number of tokens.

Strategy. As illustrated in Fig. 5, our strategy focuses on the last blocks (or the last) in the vision backbone. Here the target reduction number r could exceed half of the total tokens $\lfloor n/2 \rfloor$ in one block. We refer to this as *reduction overflow*. To handle this case, *FOLDER* automatically applies iteratively a “FOLD” operation. As detailed in Alg. 1, if reduction overflow occurs in a fold iteration (meaning that $r_{\text{remain}} > \lfloor n'/2 \rfloor$ in line 7), we reduce the tokens by half ($r_{\text{fold}} = \lfloor n'/2 \rfloor$). To do this, we first split the token input sequence into equal-sized partitions named \mathbb{A} and \mathbb{B} (line 9). Then, for each token in \mathbb{A} we identify the most similar one in set \mathbb{B} based on a Matching Function [5, 39] $S : (\mathbb{R}^d, \mathbb{R}^d) \rightarrow \mathbb{R}$ (line 10). A visual representation is provided in Fig. 5, where the “Partition & Match” operation is highlighted. These matches are then sorted based on their matching scores ($\xrightarrow{s_{ij}}$), and only the top r_{fold} matches are preserved (line 11). At this point, by merging these matches in \mathbf{M}_{top} from \mathbb{A} to \mathbb{B} , we obtain two new sets: \mathbb{A}' and \mathbb{B}' . Namely, \mathbb{B}' updates \mathbb{B} by replacing original tokens with matched tokens aggregated using a specific Aggregation Method (Sec. 3.3). \mathbb{A}' , instead, contains the tokens in \mathbb{A} whose matches were discarded in line 11. Clearly, if the reduction overflow occurs, $r_{\text{fold}} = \lfloor n'/2 \rfloor$ and thus $\mathbb{A}' = \emptyset$ (“First Fold” of Fig. 5). The concatenation between \mathbb{A}' and \mathbb{B}' represents the input token sequence for the next “FOLD” iteration, in which r_{remain} tokens are going to be removed. This process continues through successive folds (line 3) until the overflow is no longer encountered. In this case, $r_{\text{fold}} = r_{\text{remain}}$ (line 7), and r_{remain} for the next iteration will be equal to 0 (line 8). A visual representation of this case is provided in Fig. 5 in the “Last FOLD” iteration.

Algorithm 1: *FOLDER* applied in one block

Input: Token sequence $\mathbf{X} \in \mathbb{R}^{n \times d}$, reduced num r
Output: Reduced token sequence $\mathbf{X}' \in \mathbb{R}^{(n-r) \times d}$

```

1  $r_{\text{remain}} = r$ ;
2  $\mathbf{X}' = \mathbf{X}$ ;
3 while  $r_{\text{remain}} > 0$  do
4    $\mathbf{X}', r_{\text{remain}} = \text{FOLD}(\mathbf{X}', r_{\text{remain}})$ ;
5
6 Function  $\text{FOLD}(\mathbf{X}' \in \mathbb{R}^{n' \times d}, r_{\text{remain}})$  :
7    $r_{\text{fold}} = \min(\lfloor n'/2 \rfloor, r_{\text{remain}})$ ;
8    $r_{\text{remain}} = r_{\text{remain}} - r_{\text{fold}}$ ;
9    $\{\mathbb{A}, \mathbb{B}\} \leftarrow \text{Split } \mathbf{X}' \text{ into 2 equal-sized partitions}$ ;
10   $\mathbf{M} \leftarrow \text{Compute } \{(a_i \xrightarrow{s_{ij}} b_j) \mid$ 
       $b_j = \arg \max_{b_j \in \mathbb{B}} s_{ij} = S(a_i, b_j), \forall a_i \in \mathbb{A}\}$ ;
11   $\mathbf{M}_{\text{top}} \leftarrow \text{Sort } \mathbf{M} \text{ based on } \xrightarrow{s_{ij}} \text{ \& keep Top } r_{\text{fold}}$ ;
12   $\{\mathbb{A}', \mathbb{B}'\} \leftarrow \text{Merge } \mathbb{A} \text{ to } \mathbb{B} \text{ according to } \mathbf{M}_{\text{top}}$ ;
13  return  $\text{Concat}(\mathbb{A}', \mathbb{B}'), r_{\text{remain}}$ ;

```

4. Experiments

In this section, we present the results. By using *FOLDER*, we reduce the number of visual tokens to accelerate both training and inference of MLLMs.

4.1. Evaluation & Benchmarks

Evaluation Models. We evaluate our method on various MLLMs, including image understanding models LLaVA1.5-7B/13B [54] and Minigt4v2 [6], multi-vision-tower based model MMVP [76] and video understanding model Video-LLaVA [50]. For merging strategy ablation, we evaluate on BLIP [45] for the image captioning task.

Benchmarks. To quantify the ability of accelerated MLLMs, we conduct thorough experiments on a wide range of tasks, including *Y/N tasks* like MME [24],

Table 1. **Results on LLaVA1.5 7B/13B.** We highlight the best result for each benchmark under the same reduction ratio. *Retrained to provide a fair comparison in Tab. 4.

Method	Reduct Ratio	Speed Up	MMBench EN	MM Star	MME	A-OK VQA	Hallusion Bench	MM MU	OCR VQA	SEED BenchIMG	Science QA	POPE	Avg
Original-7B	0%	1×	62.8	32.7	1338.9	78.8	35.6	32.2	52.4	60.2	68.1	79.7	55.0
Pooling	50%	1.5×	59.5	30.3	1308.6	77.1	35.3	31.7	44.8	59.2	68.0	84.0	53.7
FastV [8]		1.3×	63.3	32.4	1345.1	78.6	36.5	28.7	53.1	59.4	67.8	81.0	54.9
Turbo [39]		1.5×	60.4	30.9	1311.2	77.2	35.5	28.0	35.7	58.1	67.5	83.0	52.3
Ours		1.5×	62.4	32.1	1338.2	78.3	38.3	34.0	48.5	59.5	68.5	85.4	55.5
Pooling	66%	1.7×	57.6	29.7	1308.2	74.2	32.3	30.7	38.7	57.6	67.3	80.7	51.6
FastV [8]		1.5×	62.5	32.0	1353.2	77.7	37.4	30.0	52.6	58.3	68.2	79.3	54.6
Turbo [39]		1.7×	60.1	31.5	1301.6	78.0	34.9	24.7	34.4	57.8	67.2	85.0	52.0
Ours		1.7×	61.4	30.3	1350.0	77.9	39.2	31.3	46.1	59.7	68.3	85.4	54.8
FastV [8]	75%	1.6×	61.2	31.0	1321.6	76.6	37.5	32.0	50.8	57.2	68.1	77.7	53.9
Ours+FastV		1.7×	61.4	31.2	1325.5	78.0	39.1	32.6	48.8	59.2	68.6	82.3	54.9
Original-13B*	0%	1×	66.6	30.9	1371.1	77.0	36.1	34.0	54.9	59.4	68.8	86.4	56.3
Pooling	50%	1.5×	64.1	31.2	1316.6	76.2	35.1	30.0	54.7	57.6	69.0	85.7	55.1
FastV [8]		1.3×	66.4	31.1	1386.3	75.5	36.2	32.6	54.9	58.9	68.4	85.4	55.9
Turbo [39]		1.5×	65.0	30.6	1200.2	78.2	26.9	32.7	47.9	58.8	69.7	86.1	53.9
Ours		1.5×	65.4	31.2	1383.7	78.6	36.4	34.4	56.2	59.1	70.5	86.9	56.8
Pooling	66%	1.6×	62.8	31.0	1250.6	73.5	29.5	32.5	45.6	54.5	69.7	82.1	52.6
FastV [8]		1.5×	66.3	31.2	1352.2	75.0	35.5	32.3	54.4	58.0	68.3	83.5	55.3
Turbo [39]		1.6×	64.7	31.2	1168.3	76.3	25.9	33.3	47.9	58.5	70.5	85.5	53.6
Ours		1.6×	65.8	31.7	1366.9	77.3	33.8	35.0	52.6	58.8	70.7	86.1	56.1
FastV [8]	75%	1.6×	64.2	31.7	1321.3	74.2	36.9	31.3	53.3	56.4	68.1	82.1	54.5
Ours+FastV		1.8×	65.1	32.3	1368.6	77.8	35.3	32.0	55.2	58.8	71.1	85.8	56.2

Table 2. **Results on Minigpt4v2.** We highlight the best result on each benchmark under the same reduction ratio.

Method	Reduct Ratio	Speed Up	MMBench EN	MM Star	MME	A-OK VQA	Hallusion Bench	MM MU	POPE	SEED BenchIMG	Science QA	RealW QA	Avg
Original	0%	1×	9.2	24.4	631.4	38.5	26.4	18.7	62.3	31.8	48.6	38.8	32.1
Turbo	50%	1.3×	8.7	21.0	692.1	35.0	34.7	20.7	52.7	30.5	50.4	37.6	31.6
Ours		1.3×	9.4	22.5	710.3	38.4	34.6	24.0	56.2	31.3	50.7	38.6	33.1
Turbo	60%	1.4×	9.1	22.1	674.5	36.7	34.3	23.0	51.0	30.4	50.3	38.8	32.0
Ours		1.4×	13.8	24.3	859.9	43.8	35.6	23.1	63.3	33.7	53.5	39.9	36.2
Turbo	70%	1.6×	8.7	22.0	651.8	36.3	34.4	20.7	44.7	30.7	50.1	35.0	30.6
Ours		1.6×	9.3	22.5	666.8	37.6	35.5	22.8	56.6	31.2	51.5	37.9	32.9

HallusionBench [27], POPE [84]; *MCQ tasks* like MMBench-EN [85], CCBench [85], A-OKVQA [69], ScienceQA_IMG [59], SEEDBench_IMG [44], MMMU [86], MMStar [7], Video-MME [25], RealWorld-QA [26]; and *VQA tasks* like OCRVQA [64], MMBench-Video [21]. For BLIP, we evaluate on COCO image captioning [51]. Note that due to cost budget, we only apply LLM evaluation on VQA tasks (exact matching for the others).

Retraining. To validate the effectiveness of FOLDER in MLLM training, we leverage LLaVA1.5-13B [54]. We adopt the same training setting of LLaVA1.5-13B, and apply FOLDER during both pretraining and SFT. Training details are provided in the supplementary material.

4.2. Main Results

The following experiments reveal the effectiveness of FOLDER on different MLLMs. If not specified, we only apply FOLDER in the last layer of the visual encoder.

4.2.1. Inference Acceleration on MLLM

We evaluate FOLDER’s plug-and-play acceleration performance in inference phase on various image understanding MLLMs, including LLaVA1.5-7B, LLaVA1.5-13B [54], Minigpt4v2 [6] and multi-vision-tower based model MMVP [76]. If not specified, we evaluate MLLM’s speed-up based on the time of the first output token.

Single-Vision-Tower MLLM. In Tab. 1, we compare FOLDER with previous plug-and-play SOTA [8, 39] on LLaVA1.5. Overall, FOLDER achieves the best performance-speed trade-off, comparable to or even exceeding the original performance with over 50% reduction on several benchmarks. Compared to Turbo [39], which employs uniform merging across the vision encoder, our approach demonstrates superior performance across the majority of benchmarks under the same reduction ratio. This advantage is particularly pronounced in visually dense tasks such as OCRVQA, where our method significantly outperforms Turbo. This result well accords with our preliminary observation: instead of progressive reduction, tokens should

Table 3. Results on MMVP (MLLM with Multiple Vision-towers (CLIP+DINOv2)).

Method	Reduct Ratio	Speed Up	MMBench EN	MM Star	MME	Hallusion Bench	OCR VQA	MM MU	POPE	SEED BenchIMG	Science QA	CC Bench	Avg
Original	0%	1×	64.2	32.1	1403.6	46.3	53.3	34.2	86.7	60.6	70.0	18.8	51.6
Turbo [39]	50%	1.5×	62.8	32.0	1352.9	44.0	47.6	34.0	85.6	58.6	69.1	17.9	50.0
Ours		1.5×	63.0	32.1	1362.3	46.2	50.5	34.7	85.7	59.5	70.4	18.6	50.9
Turbo [39]	66%	1.7×	62.5	30.7	1341.8	46.2	46.6	33.3	84.9	58.1	69.7	18.8	49.9
Ours		1.7×	63.6	31.9	1368.2	47.9	47.2	34.0	85.3	58.7	70.7	19.6	50.8

Table 4. Training with FOLDER. w/ F: We plug FOLDER into LLaVA1.5-13B during training (Train Reduct>0) and inference (Infer Reduct>0). Training with FOLDER yields an all-round enhancement on both performance and speed.

Train	Train Reduct	Infer Reduct	Speed Up	MMBench EN	MM Star	MME	A-OK VQA	Hallusion Bench	OCR VQA	SEED BenchIMG	Science QA	POPE	Avg
w/o F	0%	0%	(1,1)×	66.6	30.9	1371.1	77.0	36.1	54.9	59.4	68.8	86.4	58.8
w/ F	0%	66%	(1,1.6)×	65.8	31.7	1366.9	77.3	33.8	57.6	58.8	70.7	86.1	59.0
w/ F	66%	0%	(1.5,1)×	66.6	32.0	1407.7	78.9	42.8	57.7	60.9	69.3	88.3	60.8
w/ F	66%	66%	(1.5,1.6)×	67.8	32.5	1393.4	79.5	43.6	57.9	61.3	71.5	86.9	61.2
w/ F	75%	0%	(1.7,1)×	63.3	30.7	1359.5	79.1	37.7	56.2	60.2	65.6	87.8	58.8
w/ F	75%	75%	(1.7,1.8)×	65.2	30.7	1325.7	79.5	34.4	52.3	59.5	67.4	87.2	58.2

be reduced only in the last blocks.

Despite FastV [8] demonstrating comparable performance with FOLDER on some benchmarks, due to its limitations described in Sec. 2, it’s inherently slower and does not provide acceleration support for training. FOLDER, on the other hand, is a ready-to-use plug-and-play module that integrates seamlessly into the vision backbone with minimal adjustment. By directly reducing visual tokens before interfacing with the LLM, FOLDER effectively mitigates issues associated with complex LLM architectures. Note that FOLDER and FastV address token reduction from two distinct perspectives (visual redundancy and task-oriented attention). Thus, as shown in Tab. 1, coupling FOLDER with FastV (50% × 50%) can achieve additional reduction while maintaining competitive performance.

In Tab. 2, we also evaluate FOLDER on another MLLM: Minigt4v2. With a reduction ratio up to 60%, our method achieves an overall performance improvement compared to the original model, with an increase of more than 40% on MME and MMBench. Even in this case, by merging in the last block, FOLDER outperforms Turbo. This implies that, in addition to speed enhancement, FOLDER can potentially be a plug-and-play performance booster, reducing the noise occurring in long token sequences.

To prove the effectiveness of our algorithm, we also replaced the matching function [39] with a naive mean pooling operation between two partitions. The result in Tab. 1 demonstrates the superiority of matching over pooling.

Multi-Vision-Tower MLLM. Multi-vision-tower-based models [40, 72, 76] enhance MLLMs’ visual ability but aggravate the length issue. This makes our method particularly advantageous in this context. In Tab. 3 we evaluate on MMVP [76] with CLIP [66] and DINOv2 [65] as vision towers. By applying FOLDER, we trade a significant reduction in image token length (from 1152 to 576/384) with

Table 5. Results on VideoLLaVA.

Method	Reduct Ratio	Speed Up	MMBench-V Overall	MMBench-V Perception	MME Video
Original	0%	1×	1.04	1.04	31.8
Turbo	65%	2.5×	1.00	0.99	29.8
Ours		2.4×	1.04	1.05	31.9
Turbo	75%	2.8×	0.98	0.98	29.0
Ours		2.7×	1.03	1.04	30.7

an acceptable drop. Note that MMVP is trained by interleaving vision tower features, which may cause positional confusion. Despite that, FOLDER still achieves a satisfying acceleration-performance trade-off.

Video Understanding MLLM. Video-based MLLMs [30, 47, 50] can generate sequences exceeding 2000 tokens for a few frames, limiting their applicability. In Tab. 5, we show that, by applying FOLDER on Video-LLaVA, we can reduce visual tokens up to 65%, without any performance degradation. These sequences can be further reduced up to 75%, with a very slight & acceptable drop on some benchmarks. Note that we speed up the inference by 2.7× by reducing 75% visual tokens, and the result is still much better than Turbo with 66% reduction ratio.

4.2.2. Training Acceleration on MLLM

As an universal plug-and-play module for MLLM, FOLDER can be seamlessly integrated into MLLM pre-training and SFT. We conduct such an experiment on LLaVA1.5-13B, providing results in Tab. 4. Surprisingly, when incorporating FOLDER with a 66% reduction ratio, LLaVA-1.5-13B exhibits comprehensive improvements across all benchmarks, even including visually dense tasks such as OCRVQA (↑3%) and visually demanding evaluations like the Hallusion Bench (↑7.5%). These results suggest the presence of potential low-frequency noise within the visual sequence. By merging similar visual tokens, we

Table 6. **Acceleration For Training & Inference.** We evaluate training (A100-80G GPU hours) and inference acceleration (on 1st-token) on llava1.5-13B. The memory is evaluated by its peak value on H20 with batch-size 40. Note that FastV [8] can only be used during inference.

Method	Reduct Ratio	Train		Inference		
		Time(h)	Speed Up	Time(s)	Speed Up	Mem
Original	0%	187	1×	0.365	1×	81.4G
FastV		–	–	0.275	1.3×	81.4G
Turbo	50%	139	1.34×	0.250	1.5×	56.6G
Ours		141	1.33×	0.250	1.5×	56.6G
FastV		–	–	0.255	1.4×	81.4G
Turbo	66%	123	1.52×	0.230	1.6×	48.6G
Ours		124	1.51×	0.230	1.6×	48.7G
FastV		–	–	0.225	1.6×	81.4G
Turbo	75%	112	1.67×	0.205	1.8×	44.6G
Ours		113	1.65×	0.205	1.8×	44.7G

Table 7. **Ablation Study on Merging Position.** For BLIP [45], we evaluate different merging positions on layers under the image captioning task. Last- n refers to uniform reduction in last n blocks, uniform refers to uniform reduction in every block.

Method	Reduct Ratio	Throughput im/s	Speed Up	CIDEr	B@4
Original	0%	22.1	1×	133.3	39.7
Uniform		40.2	1.82×	128.8	37.9
Last-3	60%	38.4	1.74×	129.5	38.2
Last-2		37.9	1.71×	129.4	38.2
Last-1		37.5	1.71×	132.2	39.0
Uniform		47.4	2.14×	127.2	37.5
Last-3	70%	44.2	2.00×	128.4	38.2
Last-2		43.7	1.98×	130.1	38.4
Last-1		43.4	1.96×	131.0	38.9

effectively smooth this low-frequency noise, thereby enhancing the model’s learning process. Moreover, as noted in [8], attention sparsity on visual tokens is observed in the LLM attention layers, highlighting the need to reduce visual sequence length to make the model more “focused”. Furthermore, training on a reduced sequence does not compromise flexibility during inference; the original sequence can still be used at inference time, yielding improved results on certain tasks. Similarly to masked augmentation [28], FOLDER acts as a regularization mechanism. However, unlike random dropping, which is limited to the training phase, FOLDER can leverage the same aggregation framework to accelerate both training and inference.

Evaluation for Speed & Memory. On LLaVA1.5-13B, Tab. 6 tests FOLDER’s acceleration during training and inference. We train the model on 8 A100-80G and do inference on H20-96G. By reducing 66% of the tokens, we speed up the training by 1.5× and enjoy 1.6× acceleration during inference. Additionally, unlike FastV, which prunes visual tokens within the LLM, FOLDER reduces the visual tokens before the LLM, thereby significantly lowering peak mem-

Table 8. **Ablation Study on Aggregation Operation.** On BLIP [45] captioning task, we test the performance of 3 aggregation operations discussed in Sec. 3.3. For fair comparison, we adopt the aggregation only in the last block.

Method	Reduct Ratio	B@4	CIDEr	SPICE
Original	0%	133.3	39.7	23.8
Avg	50%	132.0	39.0	23.6
Drop		130.0	38.7	23.3
Weighted		132.2	39.1	23.6
Avg	60%	131.0	38.9	23.5
Drop		128.9	38.2	23.1
Weighted		131.5	39.1	23.4

ory consumption. In tests conducted with a batch size of 40 on an H20-96G, FOLDER achieves a 40% memory savings at a 66% reduction ratio. This method ideally allows for an increase in maximum batch size which amounts to 3× for a 66% reduction-particularly advantageous for training.

4.3. Ablation Study

We conduct ablation studies on BLIP [45] for image captioning task, to illustrate the idea of merging position and aggregation method discussed in Sec. 3.

Merging Position. As discussed in Sec. 3.2, we conduct experiments on the merging position, namely in which block we should merge the tokens. According to preliminary tests on ViT (Fig. 2, Fig. 3), we find out that due to the propagation effect and the decreasing trend of reduction impact, we should reduce more tokens in the last blocks rather than early blocks. Following this observation, we choose 4 different merging positions: uniform merging in each block and uniform merging in the last 1/2/3 blocks. In Tab. 7, we demonstrate the result on BLIP for the image captioning task. As shown in Tab. 7, merging only in the last block gives the best performance, which confirms our observation on ViT models. Note that due to the acceleration effect on the vision encoder, the speed-up effects vary slightly on BLIP. However, in MLLMs, the time consumption of the vision encoder is 10-15× inferior to LLM, thus yielding almost no difference for different merging positions.

Aggregation Method. In Sec. 3.3, we explore three distinct aggregation methods: Dropping, Average, and Weighted Average based on vector norms. As illustrated in Tab. 8, both average and weighted average merging show a clear advantage over direct dropping. This result is expected, as directly dropping tokens leads to greater information loss. To reduce module complexity, we used averaging in all MLLM experiments, as the differences are minimal.

5. Conclusion

In this paper, we introduce FOLDER, a plug-and-play module designed to efficiently reduce visual token sequences

in MLLMs. Through empirical analysis of token reduction process, we develop a strategy named FOLDER that elaborately focuses on large-scale token reduction in last network layers while optimizing information retention. Our experiments demonstrate that FOLDER serves as a dual-purpose accelerator for MLLMs: it achieves up to 70% reduction in visual tokens while delivering significant speedup factors of $1.8\times$ for inference and $1.65\times$ for training. Notably, FOLDER not only maintains but often enhances model performance across both inference and training scenarios, even for complicated tasks such as video understanding. The method’s effectiveness across various architectures and tasks demonstrates its potential as a practical solution for making MLLMs more computationally efficient without compromising their capabilities.

References

- [1] Josh Achiam, Steven Adler, Sandhini Agarwal, Lama Ahmad, Ilge Akkaya, Florencia Leoni Aleman, Diogo Almeida, Janko Altenschmidt, Sam Altman, Shyamal Anadkat, et al. Gpt-4 technical report. *arXiv preprint arXiv:2303.08774*, 2023. 1, 2
- [2] Anthropic. The claude 3 model family: Opus, sonnet, haiku, 2024. 1
- [3] Kirolos Ataallah, Xiaoqian Shen, Eslam Abdelrahman, Essam Sleiman, Mingchen Zhuge, Jian Ding, Deyao Zhu, Jürgen Schmidhuber, and Mohamed Elhoseiny. Goldfish: Vision-language understanding of arbitrarily long videos, 2024. 2
- [4] Adam Block, Dylan J Foster, Akshay Krishnamurthy, Max Simchowitz, and Cyril Zhang. Butterfly effects of sgd noise: Error amplification in behavior cloning and autoregression. *arXiv preprint arXiv:2310.11428*, 2023. 4
- [5] Daniel Bolya, Cheng-Yang Fu, Xiaoliang Dai, Peizhao Zhang, Christoph Feichtenhofer, and Judy Hoffman. Token merging: Your vit but faster. *arXiv preprint arXiv:2210.09461*, 2022. 2, 4, 5, 1, 3
- [6] Jun Chen, Deyao Zhu, Xiaoqian Shen, Xiang Li, Zechun Liu, Pengchuan Zhang, Raghuraman Krishnamoorthi, Vikas Chandra, Yunyang Xiong, and Mohamed Elhoseiny. Minigt-v2: large language model as a unified interface for vision-language multi-task learning. *arXiv preprint arXiv:2310.09478*, 2023. 2, 5, 6, 1
- [7] Lin Chen, Jinsong Li, Xiaoyi Dong, Pan Zhang, Yuhang Zang, Zehui Chen, Haodong Duan, Jiaqi Wang, Yu Qiao, Dahua Lin, et al. Are we on the right way for evaluating large vision-language models? *arXiv preprint arXiv:2403.20330*, 2024. 6
- [8] Liang Chen, Haozhe Zhao, Tianyu Liu, Shuai Bai, Junyang Lin, Chang Zhou, and Baobao Chang. An image is worth 1/2 tokens after layer 2: Plug-and-play inference acceleration for large vision-language models. *arXiv preprint arXiv:2403.06764*, 2024. 2, 3, 6, 7, 8
- [9] Mengting Chen, Xi Chen, Zhonghua Zhai, Chen Ju, Xuewen Hong, Jinsong Lan, and Shuai Xiao. Wear-any-way: Manip-
 utable virtual try-on via sparse correspondence alignment. *arXiv preprint arXiv:2403.12965*, 2024. 2
- [10] Xu Chen, Zida Cheng, Jiangchao Yao, Chen Ju, Weilin Huang, Jinsong Lan, Xiaoyi Zeng, and Shuai Xiao. Enhancing cross-domain click-through rate prediction via explicit feature augmentation. In *Int. World Wide Web Conf.*, 2024. 2
- [11] Zhe Chen, Jiannan Wu, Wenhai Wang, Weijie Su, Guo Chen, Sen Xing, Muyan Zhong, Qinglong Zhang, Xizhou Zhu, Lewei Lu, et al. Internvl: Scaling up vision foundation models and aligning for generic visual-linguistic tasks. In *Proceedings of the IEEE/CVF Conference on Computer Vision and Pattern Recognition*, pages 24185–24198, 2024. 1, 2
- [12] Haozhe Cheng, Cheng Ju, Haicheng Wang, Jinxiang Liu, Mengting Chen, Qiang Hu, Xiaoyun Zhang, and Yanfeng Wang. Denoiser: Rethinking the robustness for open-vocabulary action recognition. *arXiv preprint arXiv:2404.14890*, 2024. 2
- [13] Kanzhi Cheng, Wenpo Song, Zheng Ma, Wenhao Zhu, Zixuan Zhu, and Jianbing Zhang. Beyond generic: Enhancing image captioning with real-world knowledge using vision-language pre-training model. In *Proceedings of the 31st ACM International Conference on Multimedia*, pages 5038–5047, 2023. 1
- [14] Zida Cheng, Chen Ju, Xu Chen, Zhonghua Zhai, Shuai Xiao, Xiaoyi Zeng, and Weilin Huang. Image to multi-modal retrieval for industrial scenarios. *arXiv preprint arXiv:2305.03972*, 2023. 2
- [15] Zida Cheng, Shuai Xiao, Zhonghua Zhai, Xiaoyi Zeng, and Weilin Huang. Mixer: Image to multi-modal retrieval learning for industrial application. *arXiv preprint arXiv:2305.03972*, 2023. 2
- [16] Tri Dao. Flashattention-2: Faster attention with better parallelism and work partitioning, 2023. 2
- [17] Tri Dao, Daniel Y. Fu, Stefano Ermon, Atri Rudra, and Christopher Ré. Flashattention: Fast and memory-efficient exact attention with io-awareness, 2022. 2, 3
- [18] Jia Deng, Wei Dong, Richard Socher, Li-Jia Li, Kai Li, and Li Fei-Fei. Imagenet: A large-scale hierarchical image database. In *2009 IEEE conference on computer vision and pattern recognition*, pages 248–255. Ieee, 2009. 3
- [19] Alexey Dosovitskiy. An image is worth 16x16 words: Transformers for image recognition at scale. *arXiv preprint arXiv:2010.11929*, 2020. 3, 1
- [20] Carl Eckart and Gale Young. The approximation of one matrix by another of lower rank. *Psychometrika*, 1(3):211–218, 1936. 3
- [21] Xinyu Fang, Kangrui Mao, Haodong Duan, Xiangyu Zhao, Yining Li, Dahua Lin, and Kai Chen. Mmbench-video: A long-form multi-shot benchmark for holistic video understanding. *arXiv preprint arXiv:2406.14515*, 2024. 6
- [22] Zhiyuan Fang, Jianfeng Wang, Xiaowei Hu, Lijuan Wang, Yezhou Yang, and Zicheng Liu. Compressing visual-linguistic model via knowledge distillation. In *ICCV*, 2021. 2
- [23] Elias Frantar, Saleh Ashkboos, Torsten Hoefler, and Dan Alistarh. Gptq: Accurate post-training quantization for generative pre-trained transformers. *arXiv preprint arXiv:2210.17323*, 2022. 2

- [24] Chaoyou Fu, Peixian Chen, Yunhang Shen, Yulei Qin, Mengdan Zhang, Xu Lin, Jinrui Yang, Xiawu Zheng, Ke Li, Xing Sun, et al. Mme: A comprehensive evaluation benchmark for multimodal large language models. *arXiv preprint arXiv:2306.13394*, 2023. 5
- [25] Chaoyou Fu, Yuhan Dai, Yongdong Luo, Lei Li, Shuhuai Ren, Renrui Zhang, Zihan Wang, Chenyu Zhou, Yunhang Shen, Mengdan Zhang, et al. Video-mme: The first-ever comprehensive evaluation benchmark of multi-modal llms in video analysis. *arXiv preprint arXiv:2405.21075*, 2024. 6
- [26] Grok. Grok1.5 homepage. <https://x.ai/blog/grok-1.5v>, 2024. Accessed: 2024-11-14. 6
- [27] Tianrui Guan, Fuxiao Liu, Xiyang Wu, Ruiqi Xian, Zongxia Li, Xiaoyu Liu, Xijun Wang, Lichang Chen, Furong Huang, Yaser Yacoob, et al. Hallusionbench: an advanced diagnostic suite for entangled language hallucination and visual illusion in large vision-language models. In *Proceedings of the IEEE/CVF Conference on Computer Vision and Pattern Recognition*, pages 14375–14385, 2024. 6
- [28] Kaiming He, Xinlei Chen, Saining Xie, Yanghao Li, Piotr Dollár, and Ross Girshick. Masked autoencoders are scalable vision learners. In *Proceedings of the IEEE/CVF conference on computer vision and pattern recognition*, pages 16000–16009, 2022. 8
- [29] Wenxuan Huang, Zijie Zhai, Yunhang Shen, Shaoshen Cao, Fei Zhao, Xiangfeng Xu, Zheyu Ye, and Shaohui Lin. Dynamic-llava: Efficient multimodal large language models via dynamic vision-language context sparsification. *arXiv preprint arXiv:2412.00876*, 2024. 3
- [30] Peng Jin, Ryuichi Takano, Wancai Zhang, Xiaochun Cao, and Li Yuan. Chat-univi: Unified visual representation empowers large language models with image and video understanding. In *Proceedings of the IEEE/CVF Conference on Computer Vision and Pattern Recognition*, pages 13700–13710, 2024. 2, 7
- [31] Chen Ju, Peisen Zhao, Ya Zhang, Yanfeng Wang, and Qi Tian. Point-level temporal action localization: Bridging fully-supervised proposals to weakly-supervised losses. *arXiv preprint arXiv:2012.08236*, 2020. 2
- [32] Chen Ju, Peisen Zhao, Siheng Chen, Ya Zhang, Yanfeng Wang, and Qi Tian. Divide and conquer for single-frame temporal action localization. In *ICCV*, 2021.
- [33] Chen Ju, Tengda Han, Kunhao Zheng, Ya Zhang, and Weidi Xie. Prompting visual-language models for efficient video understanding. In *ECCV*. Springer, 2022.
- [34] Chen Ju, Peisen Zhao, Siheng Chen, Ya Zhang, Xiaoyun Zhang, and Qi Tian. Adaptive mutual supervision for weakly-supervised temporal action localization. *IEEE TMM*, 2022.
- [35] Chen Ju, Zeqian Li, Peisen Zhao, Ya Zhang, Xiaopeng Zhang, Qi Tian, Yanfeng Wang, and Weidi Xie. Multi-modal prompting for low-shot temporal action localization. *arXiv preprint arXiv:2303.11732*, 2023. 2
- [36] Chen Ju, Haicheng Wang, Zeqian Li, Xu Chen, Zhonghua Zhai, Weilin Huang, and Shuai Xiao. Turbo: Informativity-driven acceleration plug-in for vision-language models. *arXiv preprint arXiv:2312.07408*, 2023. 2
- [37] Chen Ju, Haicheng Wang, Jinxiang Liu, Chaofan Ma, Ya Zhang, Peisen Zhao, Jianlong Chang, and Qi Tian. Constraint and union for partially-supervised temporal sentence grounding. *arXiv preprint arXiv:2302.09850*, 2023. 2
- [38] Chen Ju, Kunhao Zheng, Jinxiang Liu, Peisen Zhao, Ya Zhang, Jianlong Chang, Qi Tian, and Yanfeng Wang. Distilling vision-language pre-training to collaborate with weakly-supervised temporal action localization. In *CVPR*, 2023. 2
- [39] Chen Ju, Haicheng Wang, Haozhe Cheng, Xu Chen, Zhonghua Zhai, Weilin Huang, Jinsong Lan, Shuai Xiao, and Bo Zheng. Turbo: Informativity-driven acceleration plug-in for vision-language large models. In *European Conference on Computer Vision*, pages 436–455. Springer, 2025. 2, 4, 5, 6, 7, 1, 3
- [40] Oğuzhan Fatih Kar, Alessio Tonioni, Petra Poklukar, Achin Kulshrestha, Amir Zamir, and Federico Tombari. Brave: Broadening the visual encoding of vision-language models. *arXiv preprint arXiv:2404.07204*, 2024. 1, 2, 7
- [41] Richard M Karp, Umesh V Vazirani, and Vijay V Vazirani. An optimal algorithm for on-line bipartite matching. In *Proceedings of the twenty-second annual ACM symposium on Theory of computing*, pages 352–358, 1990. 1
- [42] Zaid Khan, Vijay Kumar BG, Samuel Schuster, Xiang Yu, Yun Fu, and Manmohan Chandraker. Q: How to specialize large vision-language models to data-scarce vqa tasks? a: Self-train on unlabeled images! In *Proceedings of the IEEE/CVF Conference on Computer Vision and Pattern Recognition*, pages 15005–15015, 2023. 1
- [43] Zhenglun Kong, Peiyan Dong, Xiaolong Ma, Xin Meng, Mengshu Sun, Wei Niu, Xuan Shen, Geng Yuan, Bin Ren, Minghai Qin, Hao Tang, and Yanzhi Wang. Spvit: Enabling faster vision transformers via soft token pruning, 2022. 2
- [44] Bohao Li, Rui Wang, Guangzhi Wang, Yuying Ge, Yixiao Ge, and Ying Shan. Seed-bench: Benchmarking multimodal llms with generative comprehension. *arXiv preprint arXiv:2307.16125*, 2023. 6
- [45] Junnan Li, Dongxu Li, Caiming Xiong, and Steven Hoi. Blip: Bootstrapping language-image pre-training for unified vision-language understanding and generation. In *International conference on machine learning*, pages 12888–12900. PMLR, 2022. 4, 5, 8, 1
- [46] Junnan Li, Dongxu Li, Silvio Savarese, and Steven Hoi. Blip-2: Bootstrapping language-image pre-training with frozen image encoders and large language models. In *International conference on machine learning*, pages 19730–19742. PMLR, 2023. 2
- [47] KunChang Li, Yinan He, Yi Wang, Yizhuo Li, Wenhai Wang, Ping Luo, Yali Wang, Limin Wang, and Yu Qiao. Videochat: Chat-centric video understanding. *arXiv preprint arXiv:2305.06355*, 2023. 2, 7
- [48] Liunian Harold Li, Mark Yatskar, Da Yin, Cho-Jui Hsieh, and Kai-Wei Chang. Visualbert: A simple and performant baseline for vision and language, 2019. 2
- [49] Youwei Liang, Chongjian Ge, Zhan Tong, Yibing Song, Jue Wang, and Pengtao Xie. Not all patches are what you need: Expediting vision transformers via token reorganizations, 2022. 2

- [50] Bin Lin, Yang Ye, Bin Zhu, Jiayi Cui, Munan Ning, Peng Jin, and Li Yuan. Video-llava: Learning united visual representation by alignment before projection. *arXiv preprint arXiv:2311.10122*, 2023. 2, 5, 7
- [51] Tsung-Yi Lin, Michael Maire, Serge Belongie, James Hays, Pietro Perona, Deva Ramanan, Piotr Dollár, and C Lawrence Zitnick. Microsoft coco: Common objects in context. In *Computer Vision—ECCV 2014: 13th European Conference, Zurich, Switzerland, September 6-12, 2014, Proceedings, Part V 13*, pages 740–755. Springer, 2014. 6
- [52] Haotian Liu, Chunyuan Li, Qingyang Wu, and Yong Jae Lee. Visual instruction tuning. In *NeurIPS*, 2023. 2
- [53] Hao Liu, Matei Zaharia, and Pieter Abbeel. Ring attention with blockwise transformers for near-infinite context, 2023. 2
- [54] Haotian Liu, Chunyuan Li, Yuheng Li, and Yong Jae Lee. Improved baselines with visual instruction tuning. In *Proceedings of the IEEE/CVF Conference on Computer Vision and Pattern Recognition*, pages 26296–26306, 2024. 2, 5, 6, 1
- [55] Jinxiang Liu, Chen Ju, Weidi Xie, and Ya Zhang. Exploiting transformation invariance and equivariance for self-supervised sound localisation. In *ACM MM*, 2022. 2
- [56] Jinxiang Liu, Chen Ju, Chaofan Ma, Yanfeng Wang, Yu Wang, and Ya Zhang. Audio-aware query-enhanced transformer for audio-visual segmentation. *arXiv preprint arXiv:2307.13236*, 2023.
- [57] Jinxiang Liu, Yikun Liu, Fei Zhang, Chen Ju, Ya Zhang, and Yanfeng Wang. Audio-visual segmentation via unlabeled frame exploitation. *arXiv preprint arXiv:2403.11074*, 2024.
- [58] Jinxiang Liu, Yu Wang, Chen Ju, Chaofan Ma, Ya Zhang, and Weidi Xie. Annotation-free audio-visual segmentation. In *Proceedings of the IEEE/CVF Winter Conference on Applications of Computer Vision*, 2024. 2
- [59] Pan Lu, Swaroop Mishra, Tony Xia, Liang Qiu, Kai-Wei Chang, Song-Chun Zhu, Oyvind Tafjord, Peter Clark, and Ashwin Kalyan. Learn to explain: Multimodal reasoning via thought chains for science question answering. In *The 36th Conference on Neural Information Processing Systems (NeurIPS)*, 2022. 6
- [60] Chaofan Ma, Yuhuan Yang, Chen Ju, Fei Zhang, Jinxiang Liu, Yu Wang, Ya Zhang, and Yanfeng Wang. Diffusionseg: Adapting diffusion towards unsupervised object discovery. *arXiv preprint arXiv:2303.09813*, 2023. 2
- [61] Chaofan Ma, Yuhuan Yang, Chen Ju, Fei Zhang, Ya Zhang, and Yanfeng Wang. Attrseg: open-vocabulary semantic segmentation via attribute decomposition-aggregation. *arXiv preprint arXiv:2309.00096*, 2023.
- [62] Chaofan Ma, Yuhuan Yang, Chen Ju, Fei Zhang, Ya Zhang, and Yanfeng Wang. Open-vocabulary semantic segmentation via attribute decomposition-aggregation. *arXiv preprint arXiv:2309.00096*, 2023.
- [63] Chaofan Ma, Yuhuan Yang, Chen Ju, Fei Zhang, Ya Zhang, and Yanfeng Wang. Open-vocabulary semantic segmentation via attribute decomposition-aggregation. *NeurIPS*, 2024. 2
- [64] Anand Mishra, Shashank Shekhar, Ajeet Kumar Singh, and Anirban Chakraborty. Ocr-vqa: Visual question answering by reading text in images. In *ICDAR*, 2019. 6
- [65] Maxime Oquab, Timothée Darcet, Théo Moutakanni, Huy Vo, Marc Szafraniec, Vasil Khalidov, Pierre Fernandez, Daniel Haziza, Francisco Massa, Alaaeldin El-Nouby, et al. Dinov2: Learning robust visual features without supervision. *arXiv preprint arXiv:2304.07193*, 2023. 7
- [66] Alec Radford, Jong Wook Kim, Chris Hallacy, Aditya Ramesh, Gabriel Goh, Sandhini Agarwal, Girish Sastry, Amanda Askell, Pamela Mishkin, Jack Clark, et al. Learning transferable visual models from natural language supervision. In *International conference on machine learning*, pages 8748–8763. PMLR, 2021. 7, 1
- [67] Yongming Rao, Wenliang Zhao, Benlin Liu, Jiwen Lu, Jie Zhou, and Cho-Jui Hsieh. Dynamicvit: Efficient vision transformers with dynamic token sparsification. *NeurIPS*, 2021. 2
- [68] Yossi Rubner, Carlo Tomasi, and Leonidas J Guibas. The earth mover’s distance as a metric for image retrieval. *International journal of computer vision*, 40:99–121, 2000. 4
- [69] Dustin Schwenk, Apoorv Khandelwal, Christopher Clark, Kenneth Marino, and Roozbeh Mottaghi. A-okvqa: A benchmark for visual question answering using world knowledge. In *European conference on computer vision*, pages 146–162. Springer, 2022. 6
- [70] Yuzhang Shang, Mu Cai, Bingxin Xu, Yong Jae Lee, and Yan Yan. Llva-prumerge: Adaptive token reduction for efficient large multimodal models. *arXiv preprint arXiv:2403.15388*, 2024. 3
- [71] Dachuan Shi, Chaofan Tao, Ying Jin, Zhendong Yang, Chun Yuan, and Jiaqi Wang. Upop: Unified and progressive pruning for compressing vision-language transformers. *arXiv preprint arXiv:2301.13741*, 2023. 2
- [72] Min Shi, Fuxiao Liu, Shihao Wang, Shijia Liao, Subhashree Radhakrishnan, De-An Huang, Hongxu Yin, Karan Sapra, Yaser Yacoob, Humphrey Shi, et al. Eagle: Exploring the design space for multimodal llms with mixture of encoders. *arXiv preprint arXiv:2408.15998*, 2024. 1, 2, 7
- [73] Amanpreet Singh, Ronghang Hu, Vedanuj Goswami, Guillaume Couairon, Wojciech Galuba, Marcus Rohrbach, and Douwe Kiela. FLAVA: A foundational language and vision alignment model. In *Proceedings of the IEEE/CVF Conference on Computer Vision and Pattern Recognition*, 2022. 2
- [74] Hao Tan and Mohit Bansal. LXMERT: Learning cross-modality encoder representations from transformers. In *Proceedings of the 2019 Conference on Empirical Methods in Natural Language Processing and the 9th International Joint Conference on Natural Language Processing, EMNLP-IJCNLP, November 3-7, 2019*, 2019.
- [75] Gemini Team, Rohan Anil, Sebastian Borgeaud, Yonghui Wu, Jean-Baptiste Alayrac, Jiahui Yu, Radu Soricut, Johan Schalkwyk, Andrew M Dai, Anja Hauth, et al. Gemini: a family of highly capable multimodal models. *arXiv preprint arXiv:2312.11805*, 2023. 2
- [76] Shengbang Tong, Zhuang Liu, Yuexiang Zhai, Yi Ma, Yann LeCun, and Saining Xie. Eyes wide shut? exploring the visual shortcomings of multimodal llms. In *Proceedings of the IEEE/CVF Conference on Computer Vision and Pattern Recognition*, pages 9568–9578, 2024. 1, 2, 5, 6, 7

- [77] Haicheng Wang, Chen Ju, Weixiong Lin, Shuai Xiao, Mengting Chen, Yixuan Huang, Chang Liu, Mingshuai Yao, Jinsong Lan, Ying Chen, et al. Advancing myopia to holism: Fully contrastive language-image pre-training. *arXiv preprint arXiv:2412.00440*, 2024. 2
- [78] Peng Wang, Shuai Bai, Sinan Tan, Shijie Wang, Zhihao Fan, Jinze Bai, Keqin Chen, Xuejing Liu, Jialin Wang, Wenbin Ge, et al. Qwen2-vl: Enhancing vision-language model’s perception of the world at any resolution. *arXiv preprint arXiv:2409.12191*, 2024. 1, 2
- [79] Tiannan Wang, Wangchunshu Zhou, Yan Zeng, and Xinsong Zhang. Efficientvlm: Fast and accurate vision-language models via knowledge distillation and modal-adaptive pruning. *arXiv preprint arXiv:2210.07795*, 2022. 2
- [80] Guangxuan Xiao, Ji Lin, Mickael Seznec, Hao Wu, Julien Demouth, and Song Han. Smoothquant: Accurate and efficient post-training quantization for large language models. In *International Conference on Machine Learning*, pages 38087–38099. PMLR, 2023. 2
- [81] Senqiao Yang, Yukang Chen, Zhuotao Tian, Chengyao Wang, Jingyao Li, Bei Yu, and Jiaya Jia. Visionzip: Longer is better but not necessary in vision language models. *arXiv preprint arXiv:2412.04467*, 2024. 3
- [82] Yuhuan Yang, Chaofan Ma, Chen Ju, Ya Zhang, and Yanfeng Wang. Multi-modal prototypes for open-set semantic segmentation. *arXiv preprint arXiv:2307.02003*, 2023. 2
- [83] Yuhuan Yang, Chaofan Ma, Chen Ju, Fei Zhang, Jiangchao Yao, Ya Zhang, and Yanfeng Wang. Multi-modal prototypes for open-world semantic segmentation. *IJCV*, 2024. 2
- [84] Li Yifan, Du Yifan, Zhou Kun, Wang Jinpeng, Xin Zhao Wayne, and Wen Ji-Rong. Evaluating object hallucination in large vision-language models. In *The 2023 Conference on Empirical Methods in Natural Language Processing*, 2023. 6
- [85] Liu Yuan, Duan Haodong, Zhang Yuanhan, Li Bo, Zhang Songyang, Zhao Wangbo, Yuan Yike, Wang Jiaqi, He Conghui, Liu Ziwei, Chen Kai, and Lin Dahua. Mmbench: Is your multi-modal model an all-around player? *arXiv:2307.06281*, 2023. 6
- [86] Xiang Yue, Yuansheng Ni, Kai Zhang, Tianyu Zheng, Ruoqi Liu, Ge Zhang, Samuel Stevens, Dongfu Jiang, Weiming Ren, Yuxuan Sun, Cong Wei, Botao Yu, Ruibin Yuan, Renliang Sun, Ming Yin, Boyuan Zheng, Zhenzhu Yang, Yibo Liu, Wenhao Huang, Huan Sun, Yu Su, and Wenhua Chen. Mmmu: A massive multi-discipline multimodal understanding and reasoning benchmark for expert agi. In *Proceedings of CVPR*, 2024. 6
- [87] Hang Zhang, Xin Li, and Lidong Bing. Video-llama: An instruction-tuned audio-visual language model for video understanding, 2023. 2
- [88] Yuan Zhang, Chun-Kai Fan, Junpeng Ma, Wenzhao Zheng, Tao Huang, Kuan Cheng, Denis Gudovskiy, Tomoyuki Okuno, Yohei Nakata, Kurt Keutzer, et al. Sparsevlm: Visual token sparsification for efficient vision-language model inference. *arXiv preprint arXiv:2410.04417*, 2024. 3
- [89] Peisen Zhao, Lingxi Xie, Chen Ju, Ya Zhang, Yanfeng Wang, and Qi Tian. Bottom-up temporal action localization with mutual regularization. In *ECCV*. Springer, 2020. 2

In the supplementary material, we first provide more details about our FOLDER module and experiment setup in Sec. A. Then we offer more results on empirical studies (Sec. B.1) as well as ablation studies including the propagation effect on MLLMs (Sec. B.2) and the choice of aggregation strategies (Sec. B.3). Finally we discuss about the limitations and future work (Sec. C).

A. Implementation Details

A.1. FOLDER Architecture for MLLMs

FOLDER is designed as a plug-and-play module plugged in transformer-based vision encoders of Multi-modal Large Language Models (MLLMs), to reduce the output visual token sequence length. FOLDER is a generalized token merging module, that can adapt any matching function or aggregation methods, allowing any number of tokens to be merged in any block without constraint. More specifically, we applied FOLDER between the residual connection of attention block and the MLP. To minimize the calculation overhead for token grouping, we upgrade the bipartite soft matching [41] algorithm to meet the demand for arbitrary number of merging.

Merging Position ToMe [5] or Turbo [39] applies an uniform and progressive token merging, with constant number of reduction on each block to accelerate the vision encoder (ViT [19], CLIP [66], BLIP [45] etc.). Unlike them, we here focus on the acceleration of MLLMs, where the computational cost is concentrated in the LLM. Indeed, for LLaVA1.5-13B [54], the total time to generate the 1st-token is around 0.37s on V100-32G, while the vision encoder part is around 0.03s, which is less than 1/12. For all the experiments in the main paper, we only reduce tokens in the output layer/block of vision encoder (LLaVA1.5 [54] uses the image feature of the second last layer, while Minigt4v2 [6] uses only the last layer). The ablation on reduction partition between blocks conducted on MLLMs is provided in Tab. 9. Similar to the result on BLIP in the main paper, reducing tokens only in the last layer yields the best result, which is in line with our empirical observation.

Matching Function In FOLDER algorithm, we need to choose a matching function that can evaluate the similarity between tokens, so that we aggregate tokens with similar semantic meanings. ToMe [5] directly calculates the cosine similarity between tokens’ key value in attention calculation (K taking the mean on multi-head), while Turbo [39] leverage a more delicate matching function that considers both similarity between tokens and the semantic importance of tokens (attention contribution for the class token). For the experiment in the main paper, we adopt the matching function of Turbo, by replacing the metric of key value by token itself. To minimize the implementation effort, we offer an extremely simplified version that only evaluate the cosine

similarity between tokens in the last layer (between attention and MLP), and the performance gap is minor (please refer to the ablation studies in section B.3). This allows the adaptation to be a ready-to-use on any MLLM visual backbones.

Merging Order To realize the average merging that is independent of the folding order, we make one little adjustment. For example, if we have two folding operations, which asks for token (x_1, x_3, x_5) to be merged as x_8 in the first fold, and (x_6, x_7, x_8) to be merged in the second fold. We would like to average on $(x_1, x_3, x_5, x_6, x_7)$, without taking the merging order into account.

$$x_{\text{merge}} = \text{avg}(x_1, x_3, x_5, x_6, x_7)$$

To do this, we use a size list to note the number of tokens that contributed to obtaining the merged token (for the merged token x_8 after the first fold, the corresponding size is 3), then we weight the token by their size during the following fold (for token x_8 , we considered $3 \times x_8$ during the average computation with (x_6, x_7)):

$$x_8 = \text{avg}(x_1, x_3, x_5)$$

$$x_{\text{merge}} = (3 \times x_8 + x_6 + x_7)/(3 + 1 + 1)$$

In this way, we realize average merging regardless of the folding order. We release the code on BLIP and LLaVA. For more implementation details, please refer to the code along with this file.

A.2. Training Details of LLaVA1.5-13B

To test the effectiveness of FOLDER for training phase, we train LLaVA1.5-13B following the same procedures (pretrain-sft two-stage training, dataset, training parameters) detailed in LLaVA1.5 repository, with FOLDER inserted in the visual backbone of LLaVA1.5. The whole training process is conducted on 8 A100-80G GPUs and the GPU hour in Tab. 6 in the main paper is evaluated by the actual training time multiplying the number of GPUs.

B. More Experiments

B.1. Results on Empirical Studies

In addition to the empirical results on ViT-B, we also conduct such experiments on ViT-S and ViT-L to demonstrate the generality of such phenomenon. As shown in Fig. 6, 7, 8 and 9, on models of various sizes, the trend of Energy & EMD distance with respect to blocks is similar. Combined with the results in Tab. 9, we can conclude that merging on last layers is the best choice.

B.2. Ablation Study on Propagation Effect

In Tab. 8 of the main paper, we study the propagation effect on BLIP [45]. In Tab. 9, we offer results on LLaVA1.5-13B, with 4 different reduction partitions (keep the number

Table 9. **Propagation Effect on LLaVA1.5 7B/13B.** We evaluate different merging positions using LLaVA1.5 under 66% reduction ratio. Last-n refers to uniform reduction in last n blocks, uniform refers to uniform reduction in every block.

Method	Reduct Ratio	MMBench EN	MM Star	MME	A-OK VQA	Hallusion Bench	MM MU	OCR VQA	SEED BenchIMG	Science QA	POPE	Avg
Original-7B	0%	62.8	32.7	1338.9	78.8	35.6	32.2	52.4	60.2	68.1	79.7	55.0
Uniform	66%	60.1	31.5	1301.6	78.0	34.9	24.7	34.4	57.8	67.2	85.0	52.0
Last-3		60.9	31.1	1312.4	77.4	36.4	31.6	41.9	58.5	67.9	85.7	53.9
Last-2		61.1	30.4	1353.1	76.9	35.9	31.4	41.6	58.4	67.9	85.7	53.8
Last-1		61.4	30.3	1350.0	77.9	39.2	31.3	46.1	59.7	68.3	85.4	54.8
Original-13B	0%	66.6	30.9	1371.1	77.0	36.1	34.0	54.9	59.4	68.8	86.4	56.3
Uniform	66%	64.7	31.2	1168.3	76.3	25.9	33.3	47.9	58.5	70.5	85.5	53.6
Last-3		66.5	31.6	1369.4	77.2	34.5	34.8	50.1	58.7	70.9	86.5	55.9
Last-2		65.7	32.5	1332.0	77.2	34.6	34.5	51.7	58.6	70.3	86.0	55.9
Last-1		65.8	31.7	1366.9	77.3	33.8	35.0	52.6	58.8	70.7	86.1	56.1

Table 10. **Aggregation method on LLaVA1.5 7B/13B.** We test the performance of 3 aggregation operations. For fair comparison, we adopt the aggregation only in the last block.

Method	Reduct Ratio	MMBench EN	MM Star	MME	A-OK VQA	Hallusion Bench	MM MU	OCR VQA	SEED BenchIMG	Science QA	POPE	Avg
Original-7B	0%	62.8	32.7	1338.9	78.8	35.6	32.2	52.4	60.2	68.1	79.7	55.0
Direct Drop	66%	39.1	20.7	980.5	64.4	20.1	14.0	11.5	45.6	45.3	77.9	37.4
Weighted Avg		60.5	30.9	1332.3	77.7	38.8	31.3	46.6	59.8	68.2	85.6	54.7
Avg		61.4	30.3	1350.0	77.9	39.2	31.3	46.1	59.7	68.3	85.4	54.8
Original-13B	0%	66.6	30.9	1371.1	77.0	36.1	34.0	54.9	59.4	68.8	86.4	56.3
Direct Drop	66%	43.1	20.6	1082.6	65.5	18.2	19.3	29.9	45.8	47.3	79.5	40.8
Weighted Avg		65.3	31.3	1374.2	77.4	35.0	34.6	52.5	58.3	70.3	85.8	56.0
Avg		65.8	31.7	1366.9	77.3	33.8	35.0	52.6	58.8	70.7	86.1	56.1

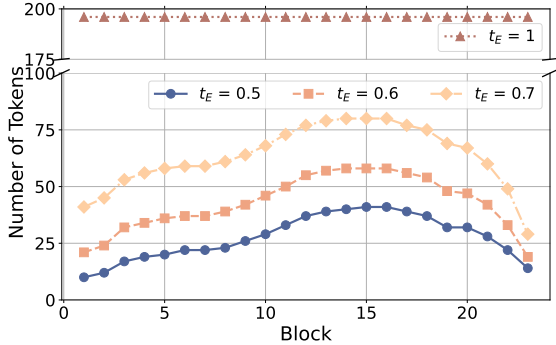


Figure 6. **Minimum Number of Tokens with Energy t_E Across Blocks on ViT Large.** We evaluate on 3 different t_E for every block on ViT large 24 blocks.

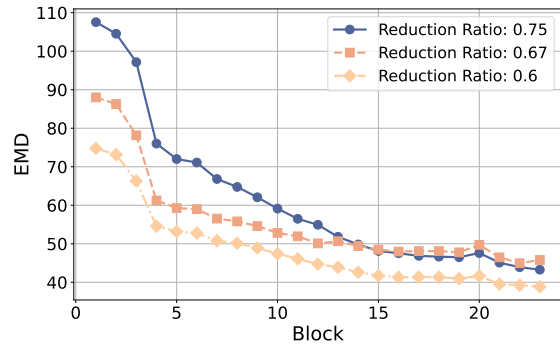


Figure 7. **EMD Distance Between Reduced and Original Output Distributions under 3 Reduction Ratios on ViT Large.** We compare the EMD distance by exerting token reduction on different blocks on ViT large 24 blocks.

of remaining tokens unchanged). Reduction in the last layer remains the best strategy for MLLMs of different sizes. Although more subtle partitions can be explored, merging only in the last layer is a simple and safe choice.

B.3. Ablation Study on Aggregation Strategy

Aggregation Method. In Tab. 10, we evaluate the three aggregation methods on MLLMs discussed in the main paper. More specifically, we conduct the experiment on

LLaVA1.5-7B and 13B to fully compare these aggregation methods. As shown in Tab. 10, there is a significant reduction in performance using direct drop, especially on dense tasks like OCRVQA. This suggests that direct drop may cause severe information loss. While for merging strategies, weighted average on norm and vanilla average merging both shows superior performance over direct dropping. The performance gap between is minor. For simplicity, we

Table 11. **Ablation for Matching Functions on LLaVA1.5 7B/13B.** We evaluate various matching functions evolved from ToMe [5] and Turbo [39]. The default setting is $\alpha = 5$ in Eq. 6 and metric as token itself. Metric = K means that we use the key value to calculate cosine similarity between tokens.

Method	Reduct Ratio	MMBench EN	MM Star	MME	A-OK VQA	Hallusion Bench	MM MU	OCR VQA	SEED BenchIMG	Science QA	POPE	Avg
Original-7B	0%	62.8	32.7	1338.9	78.8	35.6	32.2	52.4	60.2	68.1	79.7	55.0
$\alpha = 0$	66%	60.9	30.7	1354.1	76.9	39.2	31.5	45.3	59.8	68.0	85.9	54.7
$\alpha = 3$		60.8	30.7	1341.4	77.7	39.1	31.2	46.4	59.8	68.5	85.7	54.8
$\alpha = 5$		61.4	30.3	1350.0	77.9	39.2	31.3	46.1	59.7	68.3	85.4	54.8
Metric = K		61.3	30.3	1354.9	78.1	39.4	32.4	45.2	59.6	68.3	85.3	54.8
Original-13B	0%	66.6	30.9	1371.1	77.0	36.1	34.0	54.9	59.4	68.8	86.4	56.3
$\alpha = 0$	66%	65.3	31.7	1351.4	77.9	33.9	35.2	52.5	58.5	70.7	86.1	56.0
$\alpha = 3$		65.1	31.9	1383.9	77.4	34.7	34.8	52.6	58.4	70.4	86.0	56.1
$\alpha = 5$		65.8	31.7	1366.9	77.3	33.8	35.0	52.6	58.8	70.7	86.1	56.1
Metric = K		65.4	31.7	1359.5	77.8	33.1	34.0	51.4	58.2	70.9	85.4	55.6

Table 12. **Simplified Version of FOLDER on LLaVA1.5 7B/13B.** By directly applying FOLDER on the output of visual encoder, we achieve similar performance with respect to standard FOLDER, while greatly reduce the implementation effort.

Method	Reduct Ratio	MMBench EN	MM Star	MME	A-OK VQA	Hallusion Bench	MM MU	OCR VQA	SEED BenchIMG	Science QA	POPE	Avg
Original-7B	0%	62.8	32.7	1338.9	78.8	35.6	32.2	52.4	60.2	68.1	79.7	55.0
Simplified	66%	60.7	30.8	1341.1	76.4	38.8	31.6	46.4	60.1	68.4	86.3	54.7
Ours-standard		61.4	30.3	1350.0	77.9	39.2	31.3	46.1	59.7	68.3	85.4	54.8
Original-13B	0%	66.6	30.9	1371.1	77.0	36.1	34.0	54.9	59.4	68.8	86.4	56.3
Simplified	66%	65.4	31.9	1357.9	77.7	34.3	34.7	52.2	58.6	70.8	86.1	56.0
Ours-standard		65.8	31.7	1366.9	77.3	33.8	35.0	52.6	58.8	70.7	86.1	56.1

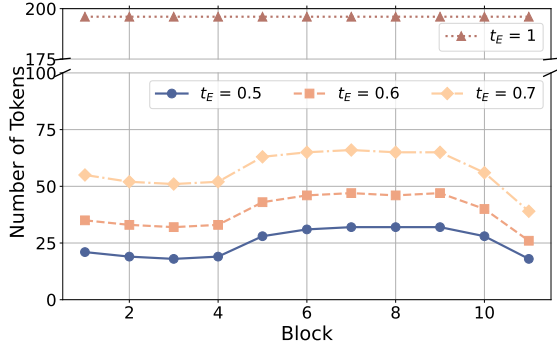


Figure 8. **Minimum Number of Tokens with Energy t_E Across Blocks on ViT Small.** We evaluate on 3 different t_E for every block on ViT small 12 blocks.

use average merging in as our default aggregation method. **Matching Function.** In addition to the aggregation method, we also conduct experiments on matching functions. Turbo [39] proposed a generalized matching function that considers both mutual redundancy (token similarity) and semantic values (attention importance), which is formulated as:

$$\mathcal{E} = \mathcal{R} - \alpha \mathcal{I}, \quad (6)$$

where \mathcal{R} the similarity between tokens and \mathcal{I} token’s attention contribution with respect to the class token. α is a

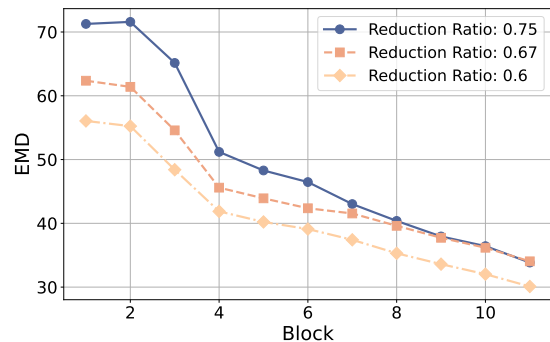


Figure 9. **EMD Distance Between Reduced and Original Output Distributions under 3 Reduction Ratios on ViT Small.** We compare the EMD distance by exerting token reduction on different blocks on ViT small 12 blocks.

weighted hyper-parameter which we take $\alpha = 5$ (a rough approximation for $\alpha = \text{seq_len} // 100$). To calculate the similarity between tokens, ToMe and Turbo [39] leverage the K (key) in the attention by taking mean on multi-head dimension, thus to save computational cost and enhance slightly the performance. In our experiment, we simply take the token itself as the metric to calculate the cosine similarity for simplicity. In Tab. 11, we ablate on different matching functions. By using various α values and metrics

on LLaVA1.5-7B and 13B, the performance rests similar, indicating the robustness of FOLDER.

Furthermore, in order to avoid all potential difficulties in implementing FOLDER (*e.g.*, FOLDER needs to be inserted into vision backbone, which requires to adapt for different vision encoder’s architecture), we introduce one extremely simplified version that only applies FOLDER on the output visual sequence from vision backbone, regardless of the model architecture. In Tab. 12, we show that such a simplified version achieves almost the same performance as standard ones, further showing the stability and universality of our proposed method.

C. Limitations & Future Work

Due to the limited resources on Openai API, for all the MLLM benchmarks (except VQA tasks that is mandatory to use LLM evaluation), we adopt exact matching, which can result in a slight degradation of actual performance evaluated by LLM. However, it’s still fair for the comparison. What’s more, the mechanism in the performance boost remains unclear, as well as a more theoretical interpretation on token reduction is yet to explore.